

Bellarmino University

ScholarWorks@Bellarmino

Undergraduate Theses

Undergraduate Works

5-13-2016

Sequencing and Analysis of a Miraculin Homolog from Two Ragweed Species

Kyj R. Mandzy

Bellarmino University, kmandzy01@bellarmino.edu

Follow this and additional works at: https://scholarworks.bellarmino.edu/ugrad_theses



Part of the [Biochemistry Commons](#)

Recommended Citation

Mandzy, Kyj R., "Sequencing and Analysis of a Miraculin Homolog from Two Ragweed Species" (2016). *Undergraduate Theses*. 4.

https://scholarworks.bellarmino.edu/ugrad_theses/4

This Thesis is brought to you for free and open access by the Undergraduate Works at ScholarWorks@Bellarmino. It has been accepted for inclusion in Undergraduate Theses by an authorized administrator of ScholarWorks@Bellarmino. For more information, please contact jstemmer@bellarmino.edu, kpeers@bellarmino.edu.

Sequencing and Analysis of a Miraculin Homolog from Two Ragweed Species

April 21
2016

Our lab has previously isolated the gene for miraculin, a taste-modifying protein, from the pollen of *Ambrosia trifida*. This weedy plant, commonly known as Giant Ragweed, is a major producer of pollen that causes hay fever. The cDNA sequence of this gene was used to design PCR primers for the amplification and sequencing of genomic DNA from this species, as well as a related species, common ragweed (*Ambrosia artemisiifolia*). These genomic sequences were analyzed in terms of intron structure, phylogenetics, and protein structure and function. These gene sequences provide novel insights into the possible roles of proteases in plants.

Kyj Mandzy
Biochemistry
Honors Thesis

TABLE OF CONTENTS

Page 2 - Introduction

Page 12 - Experimental Methods

Page 15 - Results

Page 36 - Discussion

Page 39 - Literature Cited

Introduction

The average person in an industrialized country consumes 33.1 kg of sugar a year^[3]. This accounts for a daily intake of 260 calories from sugar alone which is roughly one-eighth of the entire recommended daily caloric intake (2000 calories) the average individual needs for a day. This high intake of sugars has been implicated as one of the primary causes of obesity in the United States. Thirty-six of individuals in the United States are considered obese and a further 65% are considered overweight^[1]. These individuals face a high number of health challenges and put a large strain on healthcare service costing \$117 million annually^[6]. Neuroimaging of the brain reveals that sugar consumption results in a dopamine release in the nucleus accumbens, an area associated with motivation, novelty, and reward^[4]. Similar responses are elicited from the consumption of cocaine and heroin. Studies indicate that the responsiveness to sugars and sweetness has very ancient evolutionary beginnings^[5]. One of the proposed methods of reducing the number of individuals suffering from obesity is to exchange the amount of real sugar in foods with alternative sweeteners which would not be as calorically dense but still taste similarly.

People taste sugar with their tongues, where the molecule binds to specific receptors and triggers a sensation of sweetness. Receptors for each of the basic tastes (sweet, sour, umami, spicy, and bitter) are found in each taste bud. Sweetness is detected by a variety of G protein gustducin coupled receptors found on the taste buds^[7]. Incoming sweet molecules bind to their receptor and cause a conformational change in the molecule. The change activates the gustducin, which in turn, activates adenylate cyclase, catalyzing the conversion of ATP to cAMP. The cAMP molecule then

ultimately closes a potassium ion channel through an enzymatic cascade^[7]. The concentration of excess potassium ions increases inside the cytoplasm and depolarizes the cell, which causes a release of dopamine, which is then received by a primary afferent neuron^[7]. The individual then perceives a sweet taste. Measurement of this perceived sweetness is based on sucrose, with all sweeteners rated relative to that sugar. Sucrose has a sweetness index of 1 while most chemical sweeteners such as Stevia or Aspartame have sweetness indexes above two hundred^[8]. Sweet-tasting proteins like saccharin are one of the many methods of altering the perception of a substance^[2]. Taste-modifying proteins like curculin bind to the taste receptor itself and modify the taste of substances rather than simply amplifying the sensation of sweetness. These proteins would result in a different sensation of taste due to the different receptor activation.

Miraculin is a taste-modifying enzyme that is extracted from the fruit of *Synsepalum dulciferum* (Miracle fruit), a berry from West Africa. It is one of the more well-known taste-modifying proteins and is readily available for consumers to purchase. Ingestion of miraculin results in a perception of food being sweetened with a 17% sucrose solution. Miraculin induces a perceptual change which lasts an average of 20 minutes^[2]. Native miraculin appears both as a dimer and a tetramer but has only been expressed in recombinant species as a dimer. The glycosylation of the miraculin structure is essential for its taste modifying mechanism and serves to support its 3D conformation^[9]. Miraculin is classified as a Kunitz-type soybean trypsin inhibitor (STI) based on its primary protein structure. Similar to other members of this protein family, miraculin has a characteristic N-terminus, several cysteine residue disulfide bridges, and glycosylation

sites. How miraculin acts as a taste-modifying enzyme is not fully understood but the current model is based on two of its Histidines.

Miraculin is thought to have an invasive mechanism which changes the structure of taste receptors on the cells of the tongue. It is believed that one active site of Miraculin strongly binds to the taste receptor membrane, while the second active site fits into the sweet receptor site and changes its conformational shape^[10]. Molecular modeling of miraculin's interaction with the human taste bud has focused on the interaction of the T1R2-T1R3 sweetness receptor. Histidine residues 29 and 59 on miraculin are believed to be responsible for the binding of the receptor to the negatively-charged cavity of the T1R2-T1R3 receptor. Many charged residues (four arginine, three aspartic acids, two glutamic acids, and one lysine) are in proximity to the histidine 29 residue which results in such a physioelectirc environment. Mutation studies suggest that the conformation of the two histidine residues (29 and 59) are responsible for this taste-modifying behavior^[10]. Mutations of the histidine by replacing it with alanine residues, making them non-polar, generated miraculin with little to no sweetness-inducing ability^[10]. The histidine residue 29 is theorized to act as the binding agent to the taste receptor at the intersection of the two monomer subunits. Figures 1 and 2 depict the structure of miraculin as it aligns to the T1R2-T1R3 receptor and the mechanism of perceived sweetness, respectively.

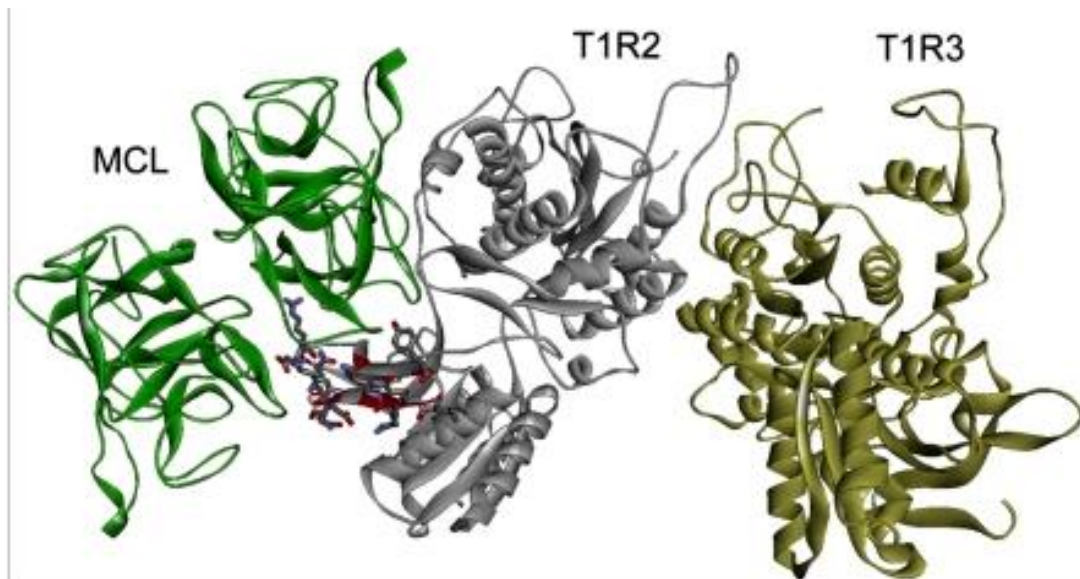


Figure 1.
Configuration of miraculin taste-modifying protein to the T1R2-T1R3 sweet-taste receptor. Koizumi, Ayako, *et al.* 2011

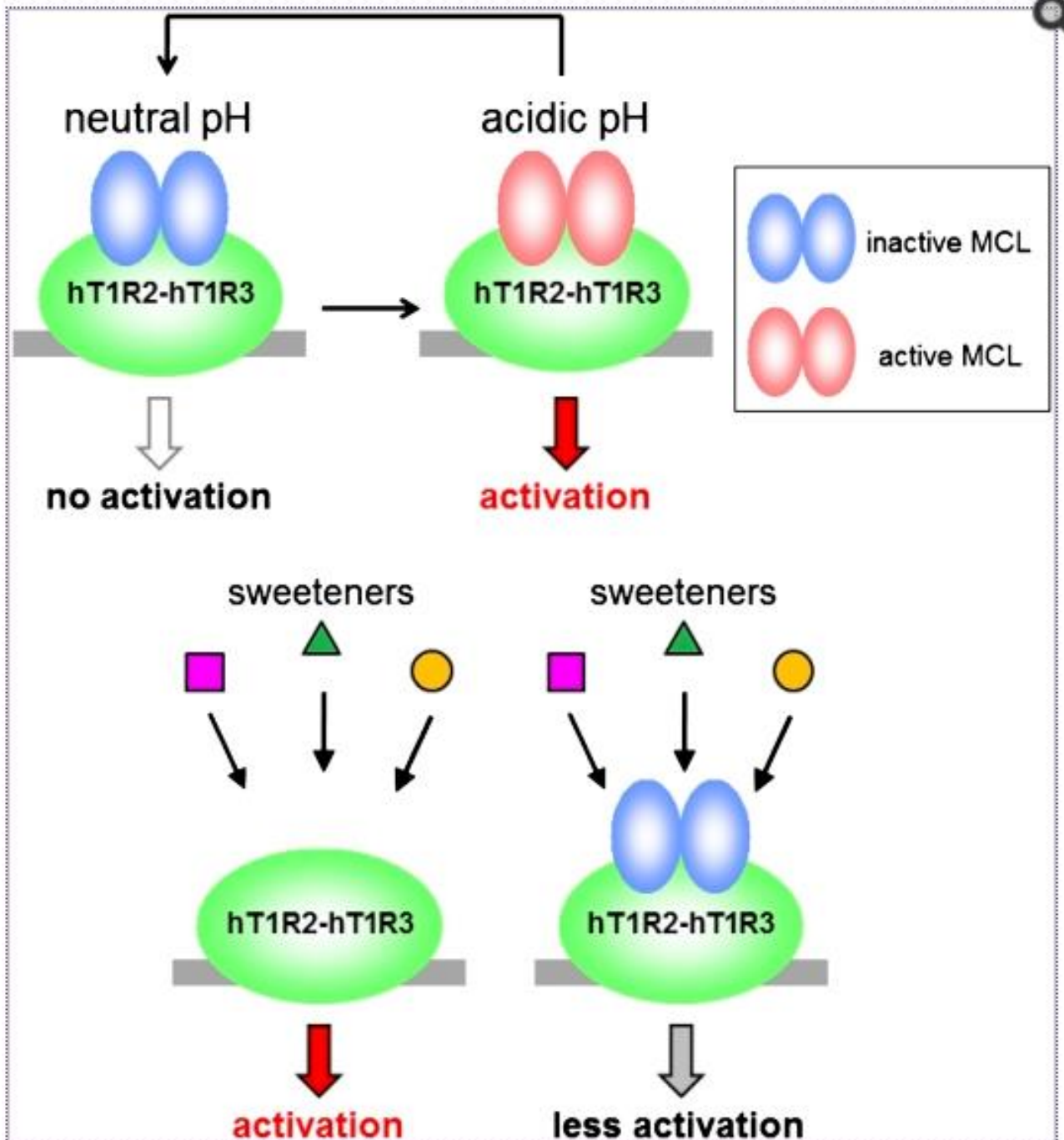


Figure 2.

Graphical representation of the interaction of the Miraculin taste-modifying protein to the T1T2-T1T3 sweet- taste receptor. Koizumi, Ayako, *et al.* 2011

There currently exists no identified genomic DNA sequence for miraculin, neither from *Synsepalum dulciferum* or any other plants. Genomic DNA refers to the sequence of nucleotides that resides within the nucleus. All published miraculin genes have been from cDNA. cDNA refers to the DNA sequence of the mRNA which makes up the codons for the amino acids in the expressed protein. cDNA lacks introns and is mostly the exons (protein coding region.) The full genomic sequencing of the DNA sequence of miraculin from ragweed would grant several insights. Currently, there exists a cDNA sequence of a giant ragweed miraculin homolog (clone # 153) collected from pollen that was isolated in the Robinson lab at Bellarmine University in the summer of 2014. That cDNA sequence presents a template for primer design with which to amplify genomic ragweed miraculin DNA. The sequencing of a variety of miraculin DNA sequences would allow analysis of gene structure, phylogenetics as well as a novel source of insight into the evolutionary development of both taste-modifying proteins and Soybean Kunitz-type trypsin inhibitor proteins^[18]. Soybean Kunitz-type trypsin inhibitor proteins function primarily as protease inhibitors, many function as either a form of protection from predators by their anti-nutritive effects, as anti-carcinogens, or simply as a component of homeostasis. However, a variety of other proteins fall into the same family based on their protein structure. Two atypical proteins of note in the Soybean Kunitz-Type family are miraculin, the taste modifying protein previously mentioned, and Lol p XI, a major grass pollen allergen^[18,19]. This implies that the research may yield information which identifies the miraculin homolog as either a potential allergen or perhaps even as a novel anti-carcinogen^[17].

Kunitz-Type Soybean trypsin inhibitors refer to a family of peptidase inhibitors. Exclusively found within Eukarya, two subfamilies exist: I3a and I3b. The I3a nomenclature refers to soybean trypsin inhibitors while I3b nomenclature refers to proteinase B type inhibitors. Both subfamilies are highly similar and are simply historically different; contemporary BLAST analysis has shown them to be 98% identical. The peptidase family I3 falls within the IC peptidase clan and is characterized by a specific Beta-trefoil^[24] fold found within all of the species of inhibitors. The two subfamilies have differing disulfide bond patterns; however, both share the same reactive sites bound in a singular disulfide bond. The ability of the I3 protein family to inhibit multiple peptidases implies that structurally dissimilar peptidases can be inhibited by a single mechanism.

In regards to inhibitory protein families, there are two major types of interactions: 1) trapping reactions, which upon the cleavage of an internal peptide bond in the inhibitor triggers a conformational change that alters the ability of the inhibitor to function by keeping it bound to the inhibitor, and 2) reversible tight-binding interactions, when the inhibitor has a high-affinity for the active site of the target enzyme^[24]. The tight-binding interaction is the more well-known mechanism and is referred to in literature as the standard mechanism. The inhibitory unit of a standard mechanism inhibitor has a single reactive-site peptide bond, and inhibition is caused by the binding of the inhibitor to the enzyme in a substrate-like fashion. Crystallographic structures of enzyme–inhibitor complexes show that the I3 family of proteins employs the standard mechanism of inhibitors^[24].

The Soybean Kunitz-type inhibitors (peptidase class inhibitor I3) has been reported to have overlapping inhibitory sites for trypsin and papain, which imply a modular means of creating an inhibitory effect to the target proteinase. The reactive-site loops, resulting from the disulfide bridges found within the reactive site, are able to adopt the canonical conformation, which inhibit serine endopeptidases by the standard mechanism, but can be altered to match a wide variety of target ligands by the supporting scaffold structures of Kunitz-Type STI's. Figure 3, depicts the reactive loops found in I3a and I3b.

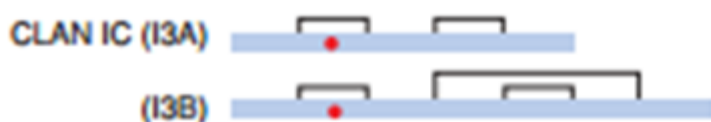


Figure 3.

Kunitz-Type STI conserved domain structures for both the I3a and I3b subfamilies. The disulfide bridges appear twice in the I3a subfamily and thrice in the I3b subfamily. The reactive loop site is represented by the red dot.
Rawlings, Neil D., Dominic P. Tolle, and Alan J. Barrett 2004

The Beta-Trefoil structure, by which proteins are placed into the Kunitz-STI superfamily, was first observed in Soybean trypsin inhibitors^[24]. The trefoil consists of 12 strands of Beta sheets forming six hairpin structures, three of the hairpins then form a central barrel structure and three other hairpins form a triangular arrangement on one side. The resulting Y-shape shows an emerging Pseudo-3 fold axis which suggests that the gene emerged from the triplication of a singular trefoil unit. The trefoil units are then able to align into greater complex which allows for inhibition due to tight-binding to the substrate.

The triangular arrangement of the three hairpins is formed by hydrogen bonding. The coiling of the Beta sheets results in the inner strands of the trefoil closest to the 3-

fold axis to form hydrogen bonds with each other. The outermost Beta-sheet coils are only able to form hydrogen bonds with the inner triangle and not with each other. This symmetrical arrangement is made possible by two hydrogen bond pairs at each level, resulting in a total of four pairs of hydrogen bonds on each inner strand. The loops forming the triangular alignment correspond with 70% of the total surface of the protein with each loop varying wildly in size and sequence. While the Kunitz STI superfamily greatly shares the tertiary structure of the Beta-Trefoil, the overall primary and secondary structure differs greatly between individual inhibitors.

The side chains of the Beta-sheet amino acids are grouped in the alignment of the layers of the Beta-Trefold, the inner Beta-sheet alignment within the Beta-trefoil the outer two layers being generally composed of a variety of side chains, each being buried in the overall structure. The innermost layer is primarily composed of hydrophobic residues with a great deal of larger residues such as Tryptophan and Phenylalanine resulting in steric conditions which most likely benefit the interlocking of the Beta-Trefold by allowing the formation of the hydrogen bonds on the outside of each inner Beta-sheet coil. Figures 4 and 5 show the structure of the Beta-Trefoil and the hydrogen bonds necessary for its construction.

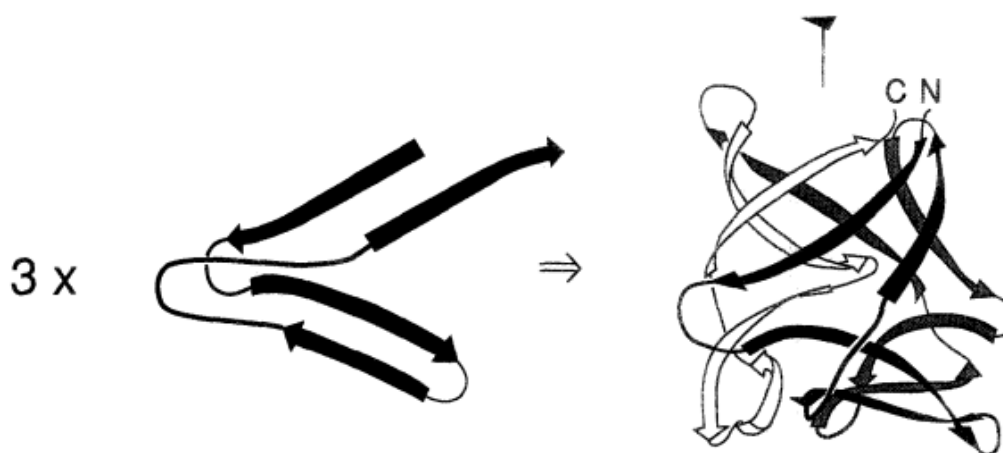


Figure 4. Lebeda, Frank J., *et al.* 1998

Schematic representation of the Beta-Trefoil found within the Kunitz-type STI family. The individual trefoil unit (left) combine into the compound Beta-Trefoil (right) resulting in the barrel shape arrangement.

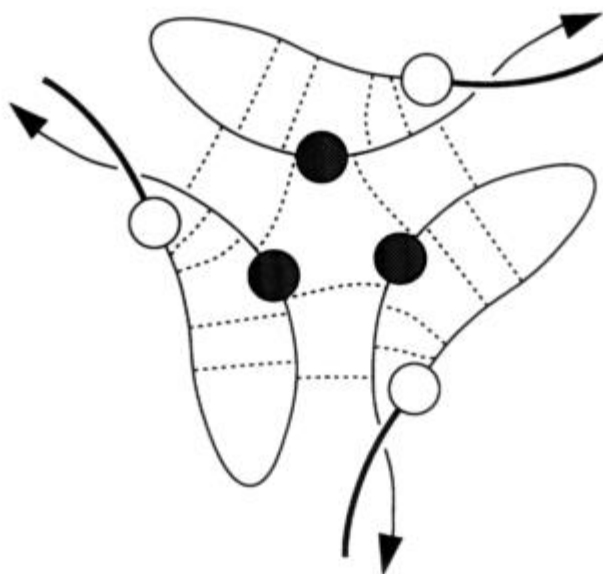


Figure 5. Lebeda, Frank J., *et al.* 1998

Schematic representation of the hydrogen bonds found within Beta-Trefoil. Four pairs of hydrogen bonds branch from each inner Beta-sheet. Two pairs align to the other two inner Beta-sheets while two simply extend to the outer Beta-sheet coils.

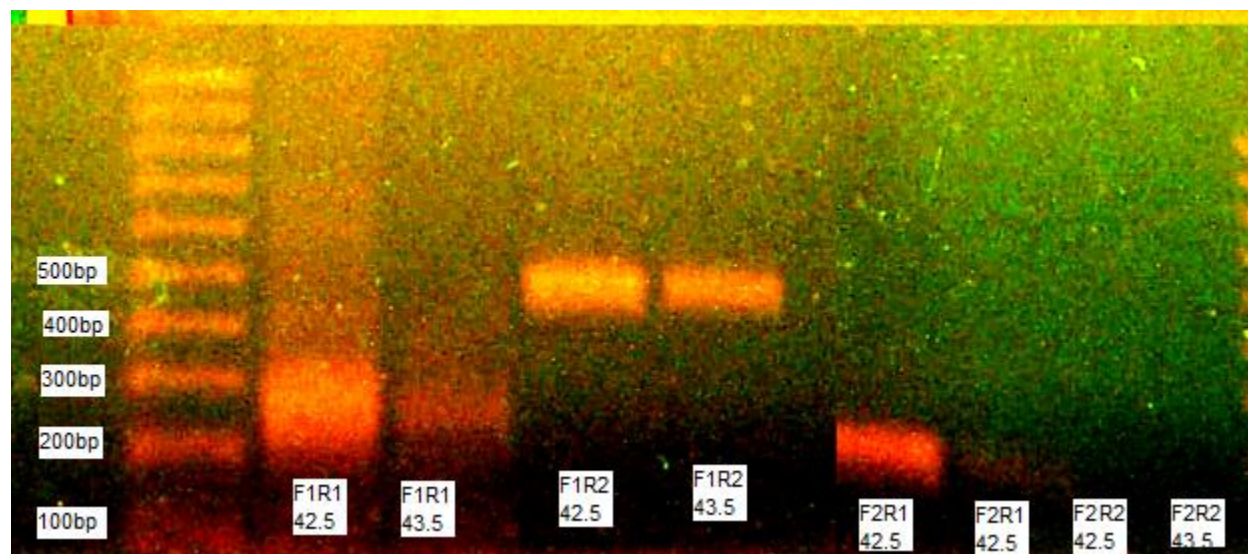
Allergen Ra3, the major allergen of Ragweed, is quite similar to miraculin and other STI proteins^[20]. Like Lol p XI (the most common form of grass allergen), it also binds to IgE and shares both disulfide bridges and Glycosylation^[19]. Ra3 binds to IgE through several disulfide bridges between its Cysteine amino acids and has a similarly active basic tail^[21].

The aim of this research in this study is to sequence and characterize the genomic DNA sequence of Miraculin homolog from *Ambrosia trifida* and the other plant species. The known cDNA sequence was used to design PCR primers to obtain the genomic DNA sequence of Miraculin. Amplified DNA was then be sequenced and analyzed. The multiple sequences were used for intron analysis, phylogenetics, and protein structure studies.

Experimental Methods

The cDNA sequence of Miraculin from *A. trifida* was used to provide a starting point for the designing of PCR primers in order to amplify the genomic DNA sequence. The sequence was utilized in a BLASTn search to find similar sequences and a consensus sequence was designed. The consensus sequence was the basis from which primers would be designed for performing PCR. Analogous annealing temperatures and purine/pyrimidine ratios were also considered in primer creation. Two pairs of primers were created, one utilizing 10 homologous plant sequences the other utilizing 12 plant sequences. Once obtained, an optimization PCR (Figure 6) was run to determine the ideal means of amplification of the genomic sequence of miraculin. Of the four different primer combinations, Primers F1 and R2 were ultimately deemed the most efficient at a 10 ng concentration of DNA and an annealing temperature of 42.5°C. The

two primers were then used to successfully run PCR for the remaining three other plants of interest *Ambrosia artemisiifolia*, *Solidago rigida*, and *Aristolochia serpentaria*. DNA was extracted from the leaves of two plant species by means of a BIORAD Nucleic Acid Extraction kit (Hercules, CA). The DNA was then amplified by PCR and purified by means of BIORAD Quantum Prep PCR Kleen kit (Hercules, CA). The DNA was then sent to the University of Louisville Biochemistry Department DNA-Core for sequencing. Once the sequences were obtained, contigs were constructed from sequences by CAP3 sequence assembly program (doua.prabi.fr/software/cap3) and trimmed for extraneous sequences. The contig nucleotide sequences were then run through BLAST searches of both the DNA sequence as well as the projected protein sequence in order to be compared to other known sequences. The NetPlantGene Server was used for intron analysis. Several other online resources were utilized: CFSSP (cho-fas.sourceforge.net/index.php) and Phyre 2.0 (<http://www.sbg.bio.ic.ac.uk/phyre2/>) to construct accurate models for the primary, secondary, and tertiary models of protein translated from the ragweed contigs.



Primers utilized for PCR amplification

Primer F1

5' CACACAACATCATGAAAAC 3'

Primer R2

5' TCCTTGCCTATTTATTATCG 3'

Figure 6.

Optimization of PCR primers with various combinations of primers shown. The combination of F1R2 at the annealing temperature of 42.5 °C resulted in the brightest bands at the requisite size.

Results

The following contigs are consensus sequences crafted from a minimum of 4 sequencing DNA reactions. The consensus sequences were constructed by CLUSTAL W alignment.

DNA Contig for Giant Ragweed

AATATTCTCATTTTCTTTAGCCCAACCCTCACCCGATGCGGTTTCGTGACATCAATGGCAACTTACTCCGATCGGGCACAACACTACTACATCCTCCCCGTCTTCAGAGGACGGGGCGGAGGCGTAACACTAGCCCCCACACGAAACGAGTCATGCCCACTTGATGTAGTCCAAGAAGGCTTCGAGCTACAGAA TGGCCTCCCCTTAACATTCACACCTGTGGATCCCAAGAAAGGCGTTATACGCGAATCCACGGATCTTAACATTATTTTTTTCGGCTTCGTCAATCTGTATTTCAGTCGAACGTTTGGATGGTTGAAGAGTACCAAGGGCAACTTATTGTTACGGGTCATGGAACGGCTGGAAACCCTGGTCAGGGAACATTAAGCAACTGGTTCAAGATAGAGAAGTATGAAGATGATTATAAGCTTGTGTTCTGTCCTACAGT

Final protein for the Giant Ragweed Contig (+2 reading frame):

TWIFSFSLAQPSDAVRDINGNLLRSGTNYIILPVFRGRGGGVTLAPTRNESCPLDV
VQEGFELQNGLP LFTFPVDPKKGVIRES TD LNIIFSASSICIQSNVWVVEEYQGQLIVTG
HGTAGNPGQGTLSNWFKIEKYEDDYKLVFCPT

DNA Contig for Common Ragweed

TTTTCTTTAGCCCAACCCTCACAGATGCGGTTTCGTGACATCAATGGCAACTTACTCCGGTCGGGCACAACTACTACATCCTCCCCGTCTTCAGAGGACGGGGCGGAGGCGTAACACTAGCCCCCACACGAAACGAGTCATGCCCACTTGATGTAGTCCAAGAAGGCTTCGAGCTACAGAATGGCCTCCCC TTAACATTCACACCTGTGGATCCCAAGAAAGGCGTTATACGCGAATCCACGGATCTTAACATTGTTTTTTCGGCTTCGTCAATCTGTATTTCAGTCGAACGTTTGGATGATTGAAGAGTACCAAGGGCAACTTATTGTTACGGGTCATGGAACGGCTGGAAACCCTGGTCAGGAAACATTAAGCAACTGGTTC AAGATAGAGAAGTATGAAGATGATTATAAGCTTGTGTTCTGTCCTACA

Final protein for the Common Ragweed Contig (+1 reading frame):

FSLAQPSDAVRDINGNLLRSGTNYIILPVFRGRGGGVTLAPTRNESCPLDVVQEGFELQNGLP
LFTFPVDPKKGVIRES TD LNIIVFSASSICIQSNVWMIIEEYQGQLIVTGHGTAGNPGQETLSNWF
KIEKYEDDYKLVFCPT

Figure 7.

Consensus sequences formed from the sequenced PCR amplified DNA sent to the UofL DNA-core and their translated protein products.

NCBI BLAST

Once the contigs were assembled, both the nucleotide contigs and the translated protein products were run through the NCBI database by BLASTn, BLASTx, and BLASTp searches. The results of which are presented below.

Giant Ragweed**BLASTn Results and Identity Percentages:**

Helianthus annuus genotype RHA276 Kunitz-like protease inhibitor 86%
Youngia japonica gene of Miraculin homolog 79%
Taraxacum officinale gene of Miraculin homolog 79%

BLASTp Results and Identity Percentages:

Kunitz-like Protease Inhibitor *Helianthus annuus* 88%
Kunitz inhibitor St1-like protein *Cynara cardunculus* 81%
Miraculin homologue *Youngia japonica* 83%
Miraculin homologue *Traxacum officinale* 84%

Common Ragweed**BLASTn Results and Identity Percentages:**

Helianthus annuus genotype RHA276 Kunitz-like protease inhibitor 86%
Youngia japonica gene of Miraculin homolog 79%
Taraxacum officinale gene of Miraculin homolog 79%

BLASTp Results and Identity Percentages:

Kunitz-like Protease Inhibitor *Helianthus annuus* 88%
Kunitz inhibitor St1-like protein *Cynara cardunculus* 81%
Miraculin homologue *Youngia japonica* 83%
Miraculin homologue *Traxacum officinale* 85%

The BLAST searches of both of the contigs yielded very similar results, with four of the same species of plants making the top matches. All four of the plants are found within the *Asteraceae* family of plants, indicating a high degree of conservation of sequence between the two plants. The BLASTx and BLASTp searches revealed the Kunitz-type STI domain present on both the Common Ragweed and Giant Ragweed sequences. Further, they both display the same reactive sites loops of the Kunitz-type STI superfamily.

Phylogenetic analysis of the nucleotide sequences results in both the common ragweed and giant ragweed bearing highest similarity to the *Helianthus annuus* Kunitz-type STI, with the miraculin-like proteins being more distantly related. This trend continues in the phylogenetic analysis of the protein sequences. The two sequences bear the greatest relationship to the *Cynara cardunuculus* Kunitz-type STI sequence, despite displaying lower BLAST identity values for the sequence. While *Youngia japonica* bears highest relatedness to the Ragweed sequences, *Traxacum officinale* was least related of the four highly similar groups. The four highly similar sequences, identified by BLAST search, were then used in the analysis of the structure of the ragweed miraculin homologues.

Intron Analysis of Contigs

During the construction of the contigs, the reading frame was found to be +1 and +2 (Giant and Common Ragweed, respectively), after translation of the contigs themselves into readable proteins. Common Ragweed contained no intron sites on either the direct or complement strands. Giant Ragweed was found to have a singular donor Intron site on the complement strand with a high confidence (0.65), but due to the nature of the

translated protein it was ruled out as a significant indicator of intron interaction. Genome sequence analysis and online prediction revealed that all KTI genes are intronless and encode proteins with a putative signal peptide for cell secretion^[27].

Donor splice sites, complement strand

Acceptor splice sites, direct strand

```

pos 5'->3' phase strand confidence 5' intron exon 3'
295 0 + 0.65 CTGTATTGAG^TCGAACGTTT

```

Figure 8..

Intron analysis of the Giant Ragweed contig by Net Plant Gene.

Comparison of the two Ragweed Contig Sequences

The two Ragweed contigs were aligned by Clustal W (Figure 9).

Common_Ragweed	-----TTTTCTTTAGCCAA	25	Common_Ragweed	CAAGAAAGGCGTTATACGCGAATCC	250
Giant_Ragweed	AATATTCTCA-----TTTTCTTTAGCCAA		Giant_Ragweed	CAAGAAAGGCGTTATACGCGAATCC	
Common_Ragweed	CCCTCACCAGATGCGGTTTCGTGACA	50	Common_Ragweed	ACGGATCTTAACATTGTTTTTCGG	275
Giant_Ragweed	CCCTCACCAGATGCGGTTTCGTGACA		Giant_Ragweed	ACGGATCTTAACATTATTTTTTCGG	
Common_Ragweed	TCAATGGCAACTTACTCCGATCGGG	75	Common_Ragweed	CTTCGTCAATCTGTATTGAGTCGAA	300
Giant_Ragweed	TCAATGGCAACTTACTCCGATCGGG		Giant_Ragweed	CTTCGTCAATCTGTATTGAGTCGAA	
Common_Ragweed	CACAACTACTACATCCTCCCCGTC	100	Common_Ragweed	CGTTTGGATGATTGAAGAGTACCAA	325
Giant_Ragweed	CACAACTACTACATCCTCCCCGTC		Giant_Ragweed	CGTTTGGATGATTGAAGAGTACCAA	
Common_Ragweed	TTCAGAGGACGGGGCGGAGGCGTAA	125	Common_Ragweed	GGGCAACTTATTGTTACGGGTCATG	350
Giant_Ragweed	TTCAGAGGACGGGGCGGAGGCGTAA		Giant_Ragweed	GGGCAACTTATTGTTACGGGTCATG	
Common_Ragweed	CCTAGCCCCACACGAAACGAGTC	150	Common_Ragweed	GAACGGCTGGAAACCTGGTCAGGA	375
Giant_Ragweed	CCTAGCCCCACACGAAACGAGTC		Giant_Ragweed	GAACGGCTGGAAACCTGGTCAGGA	
Common_Ragweed	ATGCCCACTTGATGTAGTCCAAGAA	175	Common_Ragweed	AACATTAAGCAACTGGTTCAAGATA	400
Giant_Ragweed	ATGCCCACTTGATGTAGTCCAAGAA		Giant_Ragweed	AACATTAAGCAACTGGTTCAAGATA	
Common_Ragweed	GGCTTCGAGCTACAGAATGGCCTCC	200	Common_Ragweed	GAGAAGTATGAAGATGATTATAAGC	425
Giant_Ragweed	GGCTTCGAGCTACAGAATGGCCTCC		Giant_Ragweed	GAGAAGTATGAAGATGATTATAAGC	
Common_Ragweed	CCTTAACATTACACCTGTGGATCC	225	Common_Ragweed	TTGTGTTCTGTCCTACA--	450
Giant_Ragweed	CCTTAACATTACACCTGTGGATCC		Giant_Ragweed	TTGTGTTCTGTCCTACA GT	

Figure 9.

CLUSTAL W alignment of the two Ragweed contigs. Differences between the two are highlighted in gray.

The two sequences have a total of eighteen different nucleotides that are different. Four of the differences highlighted arise from actual structural difference rather than a difference in sequence size. This indicates that the Kunitz-Type STI is highly conserved between the two species of Ragweed and further maintains the ability to utilize the modularity of the I3 superfamily in order to be able to inhibit a variety of proteases.

NCBI BLASTp was then used to align the two translated protein products against each other.

Score	Expect	Method	Identities	Positives	Gaps
294 bits(752)	1e-107	Compositional matrix adjust.	141/144(98%)	143/144(99%)	0/144(0%)
Query 6		FSLAQSPDAVRDINGNLLRSGTNYIILPVFRGRGGGVTLAPTRNESCPLDVVQEGFELQ			65
Sbjct 1		FSLAQSPDAVRDINGNLLRSGTNYIILPVFRGRGGGVTLAPTRNESCPLDVVQEGFELQ			60
Query 66		NGLPLTFTPVPDKKGVIRESTDNIIFSASSICIQSNWWMVEEYQGQLIVTGHGTAGNPG			125
Sbjct 61		NGLPLTFTPVPDKKGVIRESTDNIIFSASSICIQSNWWMVEEYQGQLIVTGHGTAGNPG			120
Query 126		QGTLSNWFKIEKYEDDYKLVFCPT			149
Sbjct 121		QETLSNWFKIEKYEDDYKLVFCPT			144

Figure 10.

NCBI BLASTp alignment of the Common and Giant ragweed (Subject and Query respectively) proteins and the consensus sequence formed between the two.

Similar to the nucleotide alignment, the two sequences bear a great deal of similarity with only three amino acids differing between the two species of ragweed. The conserved Kunitz-type Soybean Trypsin Inhibitor domain is present in both of the proteins with the reactive site loops at sites 74-81 preserved in both proteins. giant ragweed and common ragweed differ at two sites with valine and isoleucine conservative difference. Both amino acids are non-polar but their steric nature structurally different. While Ile has an extra carbon, the two amino acids branch in the

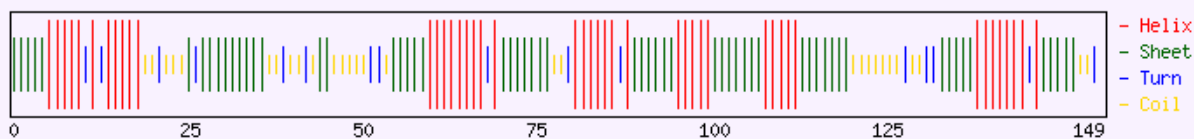
same manner. As both are hydrophobic, they are likely found in the inner coils of the Beta-sheet triangle, where their similar branching is unlikely to cause steric change significant enough to alter either the Beta-Trefoil structure or the reactive site loop. The last difference is giant ragweed contains a glycine rather than the common ragweed glutamic acid at residue 127. The difference of the non-polar to neutral charge polar amino acid could have bearing on the protein conformation, but is apparently not significant enough to cause the deformation of the Beta-Trefoil structure.

Secondary Structure Analysis

The proteins translated from the Contigs were then run through the CFSSP: Chou and Fasman Secondary Structure Prediction Server. This server produces a two dimensional picture of the Helices and Sheets for the protein. Both the Ragweed Contig translated proteins, and the four high identity proteins were analyzed by CFSSP. The results of which are presented below in Figures 11-16.

Target Sequence:

TWIFSFSLAQ PSPDAVRDIN GNLLRSGTNY YILPVFRGRG GGVTLAPTRN ESCPLDVVQE GFELQNGLPL
 TFTPVDPKKG VIRESTDINI IFSASSICIQ SNVWMVEEYQ GQLIVTGHGT AGNPGQGTLN NWFKIEKYED
 DYKLVFCPT

**Secondary Structure:**

```

      *           *           *           *           *           *
Query 1  TWIFSFSLAQPSDAVRDINGNLLRSGTNYIILPVFRGRGGGVTLAPTRNESCPLDVVQEGFELQNGLPL 70
Helix 1  HHHHHHHHHHHHHHHHHHHHHHHHHHHHHHHHHHHHHHHHHHHHHHHHHHHHHHHHHHHHHHH 70
Sheet 1  EEEEEEE                      EEEEEEEEEEE          EE          EEEEEEE  EEE 70
Turns 1  T T      T T T      T T      TT      T T      T T      70
Struc 1  EEEEEHHHHHTHTHHHHHCCTCCCEEEEEEEECCTCCTCEEECCCCCTTCEEEEEHHHHHHHHHTHEEE 70

```

```

      *           *           *           *           *           *
Query 71  TFTPVDPKKGVIRESTDINIIFSASSICIQSNVWMVEEYQGQLIVTGHGTAGNPGQGTLNWFKIEKYED 140
Helix 71  HHHHHHHHHHHHHHHHHHHHHHHHHHHHHHHHHHHHHHHHHHHHHHHHHHHHHHHHHHHHH 140
Sheet 71  EEEEE          EEEEEEEEEEE          EEEEEEEEEEEEEEEEEEE          EEEEEEE 140
Turns 71  T T T      T      T      T      T      TT      T 140
Struc 71  EEEECCTHHHHHTHEEEEEHHHHHEEEEEHHHHHEEEEEECCECCCCCTCCTTEEEEEHHHHHHHT 140

```

```

Query 141  DYKLVFCPT 149
Helix 141  HHHHH  149
Sheet 141  EEEEE  149
Turns 141  T 149
Struc 141  HEEEEECCT 149

```

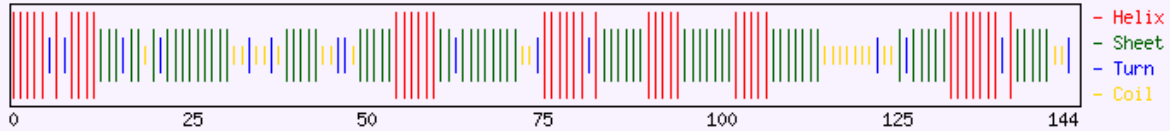
Total Residues: H: 86 E: 71 T: 21
 Percent: H: 57.7 E: 47.7 T: 14.1

Figure 11.

Secondary structure analysis of the Giant Ragweed translated protein.

Target Sequence:

FSLAQSPDA VRDINGNLLR SGTNYIILPV FRGRGGGVTL APTRNESCPL DVVQEGFELQ NGLPLTFTPV
 DPKKGVIRES TDLNIVFSAS SICIQSNVMM IEEYQGQLIV TGHGTAGNPG QETLSNWFKI EKYEYDYKLV
 FCPT

**Secondary Structure:**

```

      *           *           *           *           *           *
Query 1  FSLAQSPDAVRDINGNLLRSGTNYIILPVFRGRGGGVTLAPTRNESCPLDVVQEGFELQNGPLTFTPV 70
Helix 1  HHHHHHHHHHHHHHHHHHHHHHHHHHHHHHHHHHHHHHHHHHHHHHHHHHHHHHHHHHHHHHH 70
Sheet 1  EEEE EEEEE EEEEEEEEEEEEEEE EEEEE EEEEEEEEEEEEEEEEEEEEEEEEEEEEEEE 70
Turns 1  T T T T T T T T T T T T T T T T T T T T T T T T T T T T T T T T T 70
Struc 1  HHHHHTHTHHHEEETEECEEEEEEEEEEECCCTCCTCEEEEECCCTCEEEEEHHHHHHHEETEEEEEEEC 70

      *           *           *           *           *           *
Query 71  DPKKGVIRESTDLNIVFSASSICIQSNVMMIEEYQGQLIVTGHGTAGNPGQETLSNWFKIEKYEDDYKLV 140
Helix 71  HHHHHHHHHHHHHHHHHHHHHHHHHHHHHHHHHHHHHHHHHHHHHHHHHHHHHHHHHHHHHHH 140
Sheet 71  E EEEEEEEEE EEEEEEEEEEEEEEEEEEE EEEEEEEEEEE EEEE 140
Turns 71  T T T T T T T T T T T T T T T T T T T T T T T T T T T T T T T T T 140
Struc 71  CTHHHHHHTHEEEEEHHHHHEEEEEHHHHHEEEEECCCCCTCCETEEEEHHHHHHHTHEEEE 140

Query 141 FCPT 144
Helix 141 144
Sheet 141 E 144
Turns 141 T 144
Struc 141 ECCT 144

```

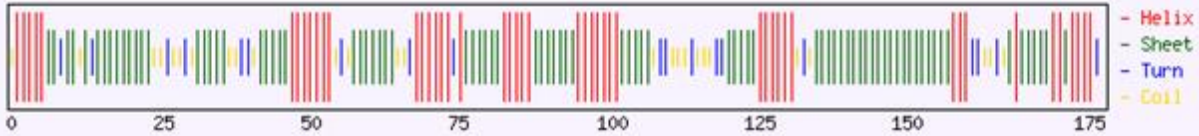
Total Residues: H: 82 E: 92 T: 21
 Percent: H: 56.9 E: 63.9 T: 14.6

Figure 12.

Secondary structure analysis of the Common Ragweed translated protein.

Target Sequence:

PDAVRDIDGN LLRSGETEYI LPVFRGRGGG VTLAPTRNES CPLDVVQEGF ELDNGLPLTF TPVDPKKGVI
 RESTDLNIIF SASSICIQSN VWMLEEYEQ RIISGRGTSG NPGGETISNW FKIEKYENGY KLVYCPTVCD
 LCRPVCGDIG VVFAENGSRRLAISDVPFKI KFRKA

**Secondary Structure:**

```

* * * * *
Query 1 PDAVRDIDGNLLRSGETEYI LPVFRGRGGVTLAPTRNESCPLDVVQEGFELDNGPLPTFTPVDPKKGVI 70
Helix 1 HHHHHH          HH              HHHHHHHHHH             HHHHH 70
Sheet 1 EEEEE EEEEEEEEEEE          EEEEE EEEEEEEEE EEEEEEE E 70
Turns 1 T T T T T T T T T T T T T T T T T T T T T T 70
Struc 1 CHHHHHEETEECCTEEEEEEEEECCTCCCEEEECCTTCEEEHMHMHHTCTEEEEEECCTHHHH 70
* * * * *
Query 71 RESTDLNIIFSASSICIQSNVWMLEEYEQRIISGRGTSGNPGGETISNWFKIEKYENGYKLVYCPTVCD 140
Helix 71 HHHHHHHHHHHHHHHHHHHHHHHHHHHHHHHHHHHHHHHHHHHH HHHHHHHHHH 140
Sheet 71 EEEEEEEEE EEEEEEEEEEEEEEEEE EEEEE EEEEEEEEE EEEEEEEEE 140
Turns 71 T T T T T T T T T T T T T T T T T T T T T 140
Struc 71 HTHEEEEEHMHHEEEEEHHHHHEEEEECTTCCCTCCCTTEEEHMHMHHTCTEEEEEEEEEE 140
* * * * *
Query 141 LCRPVCGDIGVVFAENGSRRLAISDVPFKIKFRKA 175
Helix 141 HHHHHHHH HHHHHHHHHHHHH 175
Sheet 141 EEEEEEEEEEE EEEEEEEEEEE 175
Turns 141 TT T T 175
Struc 141 EEEEEEEEEHHTTCTCEHEEEEHHEHHHT 175
  
```

Total Residues: H: 86 E: 109 T: 26
 Percent: H: 49.1 E: 62.3 T: 14.9

Figure 13.

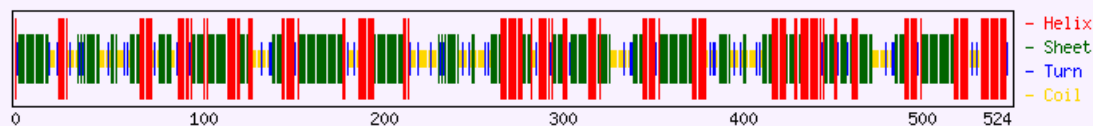
Secondary structure analysis of the *Helianthus annuus* translated protein.
 Ascension number: AFL91226

Target Sequence:

```

MKTLSLLLLF STISLCLGQP SPDPVLDIDG NLVRSGLDYY ILPVFRMG GVTLASTRNE SCPLDVVQEP
QEVNDGLPLT FTPVDPKKGV IRESTDNLII FSALSICIQS NWMLEEYEG QLIVSARGVS GNPQGETISN
WFKIEKYEDD YKIVFCPTVC DFCRPVCGDI GVIIGEDGSR RLAIIRDVPFK MKTVLLFLLF STISLSFGQK
SPDQVRDIDG NLLRSGTDYY ILPVFRGRGG GVTLAPTRNE SCPLDVVQEG FELKFGLPLK FTPVNSKKGV
IRESTDNLIM FSASTSCVQS NWMLEAYKG QLIVSGHGVW GNPQRETISN WFKIAKYEND YKLVFCPTVC
NYCKPVCEDI GVKIAENGRS HYYILPVFRG RGGVTLAPT RNECPLDVV QEGFELKFGL PLQFAPVNFK
KGVIRESDL NIFSASTCQS NWMLEAYGQL IVSGHGVWGN PGRETISNWF KIAKYENDYK LVFCPTVCNY
CKPVCGDIGV KIAENGRRL AISDVPFKVK FRKA

```



Secondary Structure:

```

      *           *           *           *           *           *
Query 1  MKTLSLLLLFSTISLCLGQPSPDPVLDIDGNLVRSGLDYYILPVFRMGGGVTLASTRNECPLDVVQEP 70
Helix 1  HHHHHHHHHHHHHH          HHHHHH          HH          HHHHHHH 70
Sheet 1  EEEEEEEEEEEEEEEEEEE          EEEEEEEEEEE          EEE          EEEEE 70
Turns 1  T          T T          T T          T          TT          T 70
Struc 1  HTEEEEEEEEEEEEEEEETCCCTHHHHCTCCCEETEEEEEEEECCCCCEEECCCTTCEEEEEHHH 70

      *           *           *           *           *           *
Query 71  QEVNDGLPLTFTPVDPKKGVIRESTDNLIIIFSALSICIQSNWMLEEYEGQLIVSARGVSGNPQGETISN 140
Helix 71  HHH          HHHHHHHHHHHHHHHHHHHHHHHHHHHHHHHHHHHHHHHHHHHHHHH 140
Sheet 71  EEEEEEE          EEEEEEEEEEEEEEEEEEEEE          EEEEEEE          EEEEE 140
Turns 71  T T          T T          T          T          T          TT 140
Struc 71  HHHCTCEEEEEEECTHHHHHHEEEEEHHHEEEEEEEEEHHHHHHHEEEHHHCCCTCCCTTEEEE 140

      *           *           *           *           *           *
Query 141 WFKIEKYEDDYKIVFCPTVCDFCRPVCGDIGVIIGEDGSRRLAIIRDVPFKMKTVLLFLLFSTISLSFGQK 210
Helix 141 HHHHHHHHHHHHHH          HHHHHHH          HHHHHHHHHHHHHHHHHHHHHHHHHHH 210
Sheet 141 EE          EEEEEEEEEEEEEEEEEEEEE          EEEEEEEEEEEEEEEEEEE 210
Turns 141 T          T T          T T          T          T 210
Struc 141 EHHHHHHHHEEEEEEEEEEEEEEEEEEEEEHHHCCCTCHHHHHHHHHHEEEEEEEEEEEEEHHHTC 210

      *           *           *           *           *           *
Query 211 SPDQVRDIDGNLLRSGTDYYILPVFRGRGGVTLAPTRNECPLDVVQEGFELKFGLPLKFTPVNSKKGV 280
Helix 211          HH          HHHHHHHHHHHHHHHHHHHHHHHHHHHHHHHHHHH 280
Sheet 211          EEEEEEEEEEE          EE          EEEEEEE          EEEEE 280
Turns 211 T T          T T          TT          T          T T 280
Struc 211 CCTCCCCCTCCCEETEEEEEEEECCCTCEEECCCTTCEEEEEHHHHHHHHHHHEEEHCCTHHH 280

      *           *           *           *           *           *
Query 281 IRESTDNLIMFSASTSCVQSNWMLEAYGQLIVSGHGVWGNPGRETISNWFKIAKYENDYKLVFCPTVC 350
Helix 281 HHHHHHHHHHHHHHHHHHHHHHHHHHHHHHHHHHH          HHHHHHHHHHHHHHHHH 350
Sheet 281 EEEEEEEEEEEEEEEEEEEEEEEEEEEEEEEEE          EEEEEEE          EEEEEEEEEEE 350
Turns 281 T T          T T          T          T TT          T 350
Struc 281 HHTHEEEEEHHHTEEEEEEEEHHHHHEHEEEEECCCCCCTCCTTEEEEEHHHHHHHTHEEEEEEEEE 350

      *           *           *           *           *           *
Query 351 NYCKPVCGDIGVKIAENGRHYYILPVFRGRGGVTLAPTRNECPLDVVQEGFELKFGLPLQFAPVNFK 420
Helix 351 HHHHHHHHH          HH          HHHHHHHHHHHHHHHHHHHHHHHHHHHHHHHHH 420
Sheet 351 EEEEEEE          EEEEEEE          EE          EEEEEEE          EEEEEEE 420
Turns 351          T TT          T T          TT          T 420
Struc 351 EEEEEEEHHHHHHHCTCTCEEEEECCCTCCEEECCCTTCEEEEEHHHHHHHEEEHHEHHHHH 420

      *           *           *           *           *           *
Query 421 KGVIRESTDNLIFSASTCQSNWMLEAYGQLIVSGHGVWGNPGRETISNWFKIAKYENDYKLVFCPTVCNY 490
Helix 421 HHHHHHHHHHHHHHHHHHHHHHHHHHHHHHHHHHHHHHHHHHHHHHHHHHHHHHHHHHH 490
Sheet 421 EEEEEEEEEEEEEEEEEEEEEEEEEEEEEEEEE          EEEEEEE          EEEEEEEEEEE 490
Turns 421 T T          T T          T TT          T 490
Struc 421 HHHHHTHEEEEEHHTEEEETHEHHHEEEEEEECCCCCCTCCTTEEEEEHHHHHHHTHEEEEEEEEEEE 490

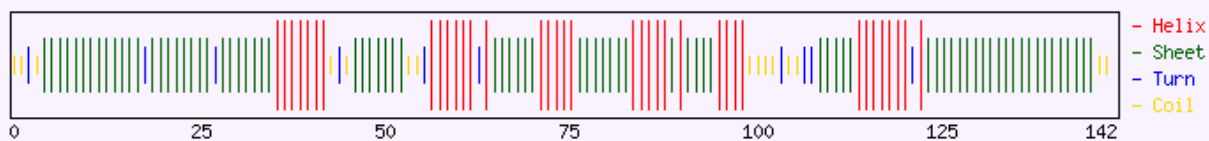
```

Figure 14.

Secondary structure analysis of the *Cynara caradunulus* translated protein. Ascension number: KVI09680

Target Sequence:

LRSGTEYYIL PVFRGMGGGL TLASTRNDTC PLDVVQADLE VDNGLPLTFT PVDPKKGIVIR ESTDLNIIFS
 ASSICIQSNV WNLEEYDQGL IVSAHGVAGN PGRETISNWF KIEKYEDDYK IVFCPTVCDF CRPVCGDIGV
 LI

**Secondary Structure:**

```

      *      *      *      *      *      *
Query 1  LRSGTEYYILPVFRGMGGGLTLASTRNDTCPLDVVQADLEVDNGLPLTFTPVDPKKGIVIRESTDNLIIFS 70
Helix 1      HH                      HHHHHHHHHH                      HHHHHHHHHHHHHHHHH 70
Sheet 1      EEEEEEEEEEEEEEEEEEEEEEEEEEEEEEEEEEEEEEEEEEEEEEEEEEEEEEEEEEEEEEEEE 70
Turns 1      T T          T          T          T          T          T T          T 70
Struc 1      CCTCEEEEEEEEEEEEEETEEEEEEEEETEEEEEEHHHHHHHCTCEEEEEEECCTHHHHHHTHEEEEEHH 70

      *      *      *      *      *      *
Query 71 ASSICIQSNVWNLEEYDQGLIVSAHGVAGNPGRETISNWFKIEKYEDDYKIVFCPTVCDFCRPVCGDIGV 140
Helix 71  HHHHHHHHHHHHHHHHHHHHHHHHHHHHHHHHHHHHHHHHHHHHHHHHHHHHHHHHHHHHHHHHH 140
Sheet 71  EEEEEEEEE EEEEEEE EEEEEEE EEEEEEEEEEEEEEEEEEEEEEEEEEEEEEEEEEEEE 140
Turns 71  T          T          T TT          T 140
Struc 71  HHHEEEEEEHHHHHEHEEEHHHHCCCTCCTTEEEHHHHHHHTHEEEEEEEEEEEEEEEEEEEEE 140

```

```

Query 141 LI 142
Helix 141 142
Sheet 141 142
Turns 141 142
Struc 141 CC 142

```

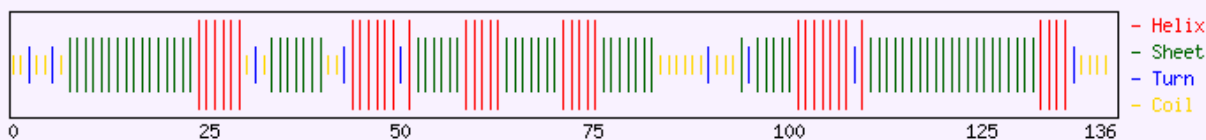
Total Residues: H: 72 E: 97 T: 15
 Percent: H: 50.7 E: 68.3 T: 10.6

Figure 15.

Secondary structure analysis of the *Youngia japonica* translated protein.
 Ascension number: BAA82840

Target Sequence:

FRGRGGVTL APTRTELCPL DVVQANQELD NGLPLTFTPV DPKKGVIRESTDLNIIFSAS SICIQSNVWM
 IEEYDGLIV SAHGVQGNPG QETLSNWFKI EKFDYKIVFCPAVCDVCR PLCGDIGVEI DENGRR

**Secondary Structure:**

```

      *      *      *      *      *      *
Query 1  FRGRGGVTLAPTRTELCPLDVVQANQELDNGLPLTFTPVDPKKGVIRESTDLNIIFSASSICIQSNVWM 70
Helix 1          HHHHHHHHHHHHHHHHHHHHHHHHHHHHHHHHHHHHHHHHHHHHHHHHHHHHHHHHHHHHH 70
Sheet 1          EEEEEEEEEEEEEEEEEEEEEEEEEEEEEEEEEEEEEEEEEEEEEEEEEEEEEEEEEEEEE 70
Turns 1          T T          T T          T T T          T          T          70
Struc 1  CCTCCTCEEEEEEEEEEEEEEEEEHHHHHHTCEEEEEEECTHHHHHHTHEEEEEHHHHHEEEEEEEHH 70

      *      *      *      *      *      *
Query 71  IEEYDGLIVSAHGVQGNPGQETLSNWFKIEKFDYKIVFCPAVCDVCRPLCGDIGVEIDENGRR 136
Helix 71  HHHH  HH          HHHHHHHHHHHHHHHHHHHHHHHHHHHHHHHHHHHHHHHHHHHHHHH 136
Sheet 71  EEEEEEEEEEE          EEEEEEEEEEE          EEEEEEEEEEEEEEEEEEEEEEEEEEE 136
Turns 71          T          T TT          T          T          T          T          136
Struc 71  HHHEEEEEEECCCCCTCCCEEEEEHHHHHHHTHEEEEEEEEEEEEEEEEEEEEEHHHHTCCCC 136

```

Total Residues: H: 78 E: 88 T: 14
 Percent: H: 57.4 E: 64.7 T: 10.3

Figure 16.

Secondary structure analysis of the *Traxacum Officinale* translated protein. Ascension number: BAA82842

Each of the proteins contain the requisite amount of Beta-sheets necessary for the construction of the Beta-Trefoil^[25] indicative of the Kunitz-Type STI. Furthermore, all of the proteins modeled contain the requisite amount of turns by which the triangular inner Beta-Trefoil and outer barrel formation may be constructed. Despite the differences in size found between the *Cynara caradunulus* and the other five protein products, the Beta-Trefoil is conserved and the reactive site which allows the Kunitz-type STI to function by tight-affinity binding. Three-dimensional modeling of the protein

sequences further confirms the maintenance of the Beta-Trefoil in each of the high-identity proteins.

Tertiary Structure Analysis and 3 Dimensional Modeling

The proteins translated from the contigs were then run through the Phyre²: Protein Homology/analogy Recognition Engine V 2.0 Server. This server produce three dimensional picture of the protein by aligning the sequence to the existing 3-D model based on identity. Both of the Ragweed Contigs translated proteins, and the four high identity proteins were analyzed by Phyre²: The results of which are presented in Figures 17-22.



Figure 17. Giant Ragweed 3D model drawn by usage of Phyre^{2.0} Server
Modeling Identity: Fold:beta-Trefoil Superfamily:STI-like
Family:Kunitz (STI) inhibitors



Figure 18. Common Ragweed 3D model drawn by usage of Phyre^{2.0} Server
Modeling Identity: Fold:beta-Trefoil Superfamily:STI-like
Family:Kunitz (STI) inhibitors

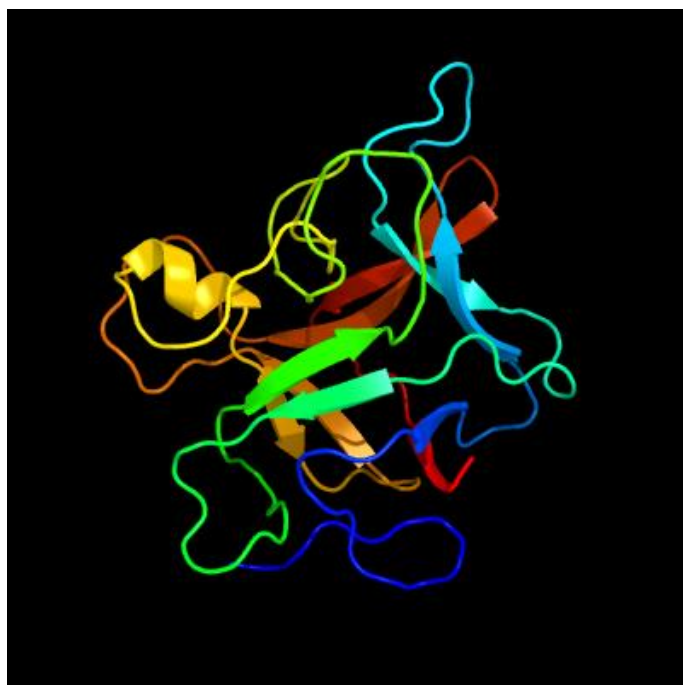


Figure 19. *Helianthus annuus* 3D model drawn by usage of Phyre^{2.0} Server
Modeling Identity: Fold:beta-Trefoil Superfamily:STI-like
Identity: crystal structure of a papaya latex serine protease inhibitor (ppi)
Ascension number: AFL91226

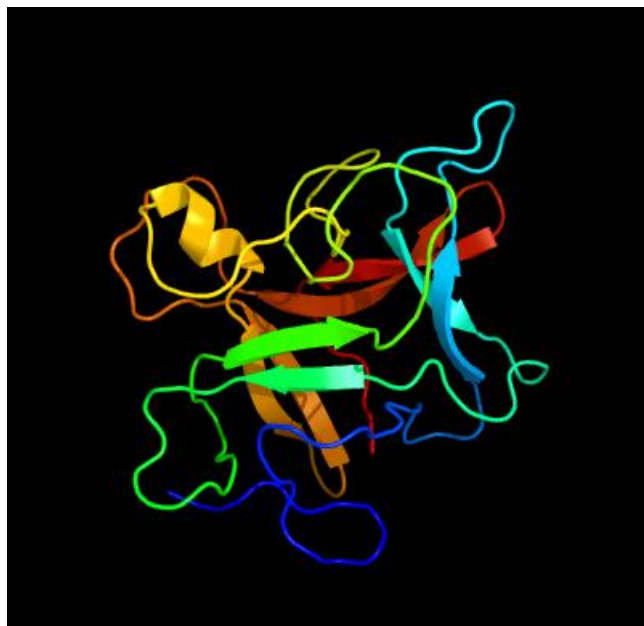


Figure 20. *Cynara cardunculus* 3D model drawn by usage of Phyre^{2.0} Server
Modeling Identity: Fold:beta-Trefoil Superfamily:STI-like
Identity: crystal structure of a papaya latex serine protease inhibitor (ppi)
Ascension number: KVI09680

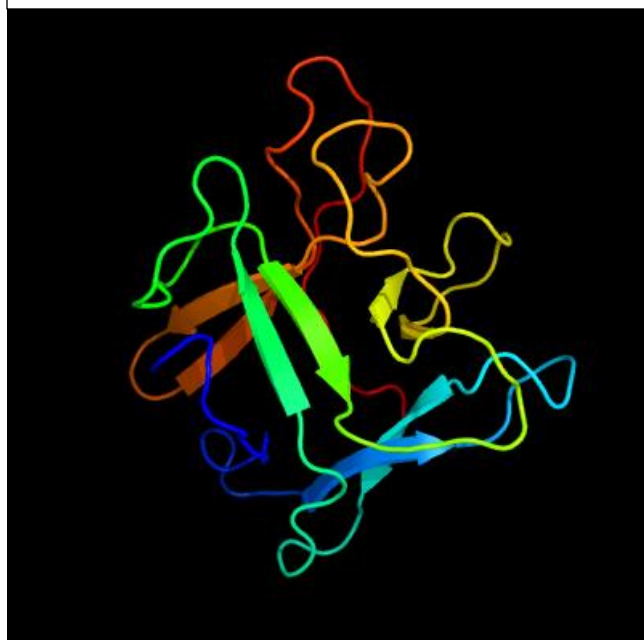


Figure 21. *Youngia japonica* 3D model drawn by usage of Phyre^{2.0} Server
Modeling Identity: Fold:beta-Trefoil Superfamily:STI-like
Identity: crystal structure of Miraculin like protein from seeds of murraya2
koenigii
Ascension number: BAA82840

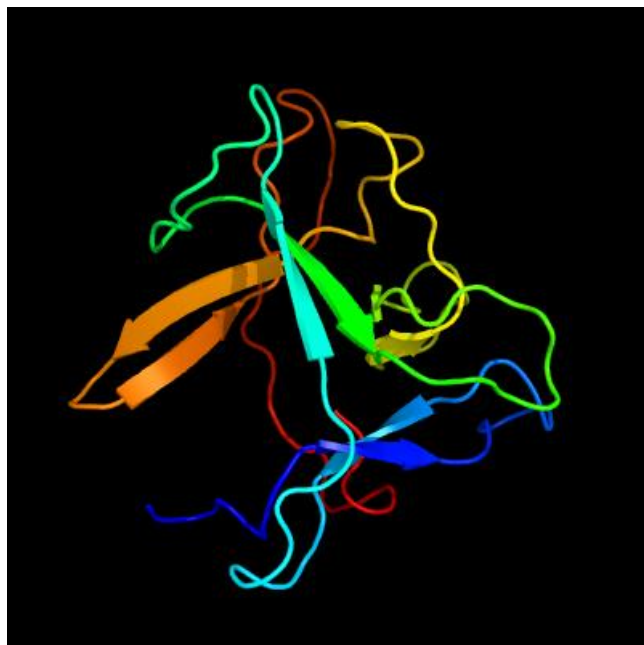


Figure 22. *Traxacum officinale* 3D model drawn by usage of Phyre^{2.0} Server
Modeling Identity: Fold:beta-Trefoil Superfamily:STI-like
Identity: crystal structure of Miraculin like protein from seeds of murraya2
koenigii
Ascension number: BAA82842

As shown by three-dimensional modeling, both the Common and Giant Ragweed proteins show the presence of the Beta-Trefoil structure. As seen in the secondary structure analysis, the proteins showed a requisite amount of Beta sheet structures from which to create the barrel. The six analyzed proteins yielded three identity-based model structures. The two Ragweed proteins, which were translated from the constructed contigs, most closely matched Kunitz-type STI. The two most phylogenetically similar proteins *Youngia japonica* and *Cynara cardunuculus* were modeled on a Papaya latex serine-protease inhibitor. The Papaya latex serine protease itself is a member of the Kunitz-type Superfamily. The two are likely to bear higher identities with the Papaya latex serine protease inhibitor due to the additional amino acid sequences outside of the Kunitz domain as the other two sequences are both longer. The other two highly proteins with high identity scores were modeled most similarly with a miraculin homologue, most likely due to the proteins themselves being miraculin homologs. Their protein models lack the post-translational modification of miraculin, the addition of four polysaccharide groups, which is likely why they still express the Beta-trefoil structure indicative of Kunitz-type STI proteins.

Ra3 Comparison

BLAST comparison of the known protein sequence of Ra3 (the major allergen of ragweed) ^[21] and the translated protein products of the ragweed contigs found no alignment between the two. It is unlikely that there is more to the similarity of the Ra3 allergen to Kunitz-Type STI's than superficial coincidence. The Ra3 protein was unable to become aligned to the translated protein products of the ragweed contigs.

Discussion

The analysis of the cDNA miraculin homolog from giant ragweed may present novel insight into the high degree of similarity between Kunitz-type Soybean Trypsin Inhibitor proteins and miraculin homologs. Miraculin falls into the Kunitz-type STI superfamily by the crystalization of its protein, before it undergoes post-translational modification and is glycosylated. This miraculin protein, when crystalized, displays the classic Beta-Trefoil^[23] of the I3 proteinase superfamily. Miraculin's structure, alongside its polysaccharide groups, has yet to be fully characterized. Existing characterization of the miraculin protein has only given the amounts of sugars attached to the miraculin protein, but their contributions to the overall structure of miraculin has yet to be determined. The amino acid sequence of miraculin contains the Kunitz domain with the reactive site loop. It is likely that the presence of polysaccharides in miraculin alters the Beta-Trefoil structure to where it is no longer able to engage in the tight-binding affinity of the I3 superfamily. Two possibilities may prevent the Beta-Trefoil structure. The first is the presence of the polysaccharide groups interfering with the steric alignment of hydrophobic phenylalanine and tryptophan within the inner coil. Both are large non-polar hydrophobic amino acids which, if displaced by the polysaccharides, would prevent the formation of the interior Beta-sheet coils necessary for the Beta-Trefoil conformation. The second possibility is replacement of the original amino acid hydrogen bonds between the inner and outer Beta-sheet coils by a polysaccharide unit. There are four pairs hydrogen bonds between each pair of coils which results in the triangular alignment of the Beta-Trefoil. The presence of numerous hydroxyl groups on polysaccharides provide an environment where a diversity of hydrogen bonds may form

in the place of the hydrogen bonds between the amino acids. The inability of the Beta-Trefoil to form would similarly prevent the reactive site loop from forming and initiating the tight-binding affinity typical to the I3 superfamily. The new conformation of miraculin may then have a conformation where the two histidines (His-29 and His-59) are able to bind to the taste-receptors in such a manner as to elicit the conformational change of the receptor resulting in the higher perceived sweetness.

In summary, the primers constructed for the amplification of both the common and giant ragweed sequences were successful. The contigs constructed from the amplified sequences had high fidelity which allowed for proper analysis of their protein products. Both the giant and common ragweed "Miraculin-homolog" fall within the I3A sub family of the Kunitz-type Soybean trypsin Inhibitors protein superfamily by the presence of their Beta-Trefoil. The conserved Kunitz-type Soybean Trypsin Inhibitor domain is present in both of the proteins with the reactive site loops at sites 74-81 being preserved in both proteins, which makes it likely that that the better classification of the original cDNA sequence would be a Kunitz-Type STI, and both proteins as protease inhibitors within ragweed, rather than taste-modifying proteins because one doesn't know if the protein would then be glycosylated in the post-translation process. The expression of these Kunitz-type STI's within ragweed is likely not limited to the pollen. Other Kunitz-type STI's in similar plants are expressed in all tissues of the plant (especially roots and stems) and that they might be helping the plant resist infection by fungi that cause disease similar plants.^[27] The miraculin-homolog identified in the cDNA likely serves a similar function.

The identity of the miraculin homolog sequences as Kunitz-type STI serves to highlight the terminological differences used in the study of plant genomics and is important in broader

terms as it may serve as a basis for the reclassification of a great deal of published sequences. Instead of erroneously publishing sequences as miraculin-homologs, future studies may seek to assess whether the sequence has the two functional histidines, which trigger a conformational change in T1R2-T1R3 taste receptors. If the sequences then lacks this reactive site and does not undergo glycosylation as a part of its post-translational modification, then it is simply a Kunitz-type STI.

Literature Cited

1. Flegal, K. M., Carroll, M. D., Kit, B. K., & Ogden, C. L. (2012). Prevalence of obesity and trends in the distribution of body mass index among US adults, 1999-2010. *Journal of The America Medical Association*, 307(5), 491-497.
2. Kurihara, K., & Beidler, L. M. (1968). Taste-modifying protein from miracle fruit. *Science*, 161(3847), 1241-1243.
3. Ismail, A. I., Tanzer, J. M., & Dingle, J. L. (1997). Current trends of sugar consumption in developing societies. *Community Dentistry and Oral Epidemiology*, 25(6), 438-443.
4. Blass, E. M. (1987). Opioids, sweets and a mechanism for positive affect: Broad motivational implications. In *Sweetness* (pp. 115-126). Springer London.
5. Adler, J., & Epstein, W. (1974). Phosphotransferase-system enzymes as chemoreceptors for certain sugars in *Escherichia coli* chemotaxis. *Proceedings of the National Academy of Sciences*, 71(7), 2895-2899.
6. Thompson, D., & Wolf, A. M. (2001). The medical-care cost burden of besity. *Obesity Reviews*, 2(3), 189-197.
7. Kinnamon, S. C. (2012). Taste receptor signalling—from tongues to lungs. *Acta physiologica*, 204(2), 158-168.
8. Joesten, Melvin D; Hogg, John L; Castellion, Mary E (2007). "Sweetness Relative to Sucrose (table)". *The World of Chemistry: Essentials* (4th ed.). Belmont, California: Thomson Brooks/Cole. p. 359. ISBN 0-495-01213-0.
9. Misaka, T. (2013, March). Molecular mechanisms of the action of Miraculin, a taste-modifying protein. In *Seminars in cell & developmental biology* (Vol. 24, No. 3, pp. 222-225). Academic Press
10. Paladino, A., Costantini, S., Colonna, G., & Facchiano, A. M. (2008). Molecular modelling of Miraculin: structural analyses and functional hypotheses. *Biochemical and biophysical research communications*, 367(1), 26-32.
11. Duhita, N., Hiwasa-Tanase, K., Yoshida, S., & Ezura, H. (2009). Single-step purification of native Miraculin using immobilized metal-affinity chromatography. *Journal of agricultural and food chemistry*, 57(12), 5148-5151.
12. Ito, K., Asakura, T., Morita, Y., Nakajima, K. I., Koizumi, A., Shimizu-Ibuka, A., ... & Abe, K. (2007). Microbial production of sensory-active Miraculin. *Biochemical and biophysical research communications*, 360(2), 407-411.
13. Mabashi, Y., Kikuma, T., Maruyama, J. I., Arioka, M., & Kitamoto, K. (2006). Development of a versatile expression plasmid construction system for *Aspergillus oryzae* and its application to visualization of mitochondria. *Bioscience, biotechnology, and biochemistry*, 70(8), 1882-1889.
14. Kanemori, Y., Gomi, K., Kitamoto, K., KUMAGAI, C., & TAMURA, G. (1999). Insertion analysis of putative functional elements in the promoter region of the *Aspergillus oryzae* Taka-amylase A gene (amyB) using a heterologous *Aspergillus nidulans* amdS-lacZ fusion gene system. *Bioscience, biotechnology, and biochemistry*, 63(1), 180-183.

15. Gomi, Kimura, Y., and Hara, S., Integrative transformation of *Aspergillus oryzae* with a plasmid containing the *Aspergillus nidulans* argB gene. *Agric. Biol. Chem.*, 51, 2549–2555 (1987)
16. Theerasilp, S., & Kurihara, Y. (1988). Complete purification and characterization of the taste-modifying protein, Miraculin, from miracle fruit. *Journal of Biological Chemistry*, 263(23), 11536-11539.
17. Kobayashi, H., Suzuki, M., Kanayama, N., & Terao, T. (2004). A soybean Kunitz trypsin inhibitor suppresses ovarian cancer cell invasion by blocking urokinase upregulation. *Clinical & experimental metastasis*, 21(2), 159-166.
18. Lee, S. I., Lee, S. H., Koo, J. C., Chun, H. J., Lim, C. O., Mun, J. H., ... & Cho, M. J. (1999). Soybean Kunitz trypsin inhibitor (SKTI) confers resistance to the brown planthopper (*Nilaparvata lugens* Stål) in transgenic rice. *Molecular Breeding*, 5(1), 1-9.
19. van Ree, R., Hoffman, D. R., van Dijk, W., Brodard, V., Mahieu, K., Koeleman, C. A., ... & Aalberse, R. C. (1995). Lol p XI, a new major grass pollen allergen, is a member of a family of soybean trypsin inhibitor-related proteins. *Journal of allergy and clinical immunology*, 95(5), 970-978.
20. Goodfriend, L., Roebber, M., Lundkvist, U., & Choudhury, A. M. (1981). Two variants of ragweed allergen Ra3. *Journal of Allergy and Clinical Immunology*, 67(4), 299-304.
21. Klapper, David G., L. Goodfriend, and J. D. Capra. "Amino acid sequence of ragweed allergen Ra3." *Biochemistry* 19.25 (1980): 5729-5734.
22. Koizumi, A., Tsuchiya, A., Nakajima, K. I., Ito, K., Terada, T., Shimizu-Ibuka, A., & Abe, K. (2011). Human sweet taste receptor mediates acid-induced sweetness of miraculin. *Proceedings of the National Academy of Sciences*, 108(40), 16819-16824.
23. Lebeda, F. J., Umland, T. C., Sax, M., & Olson, M. A. (1998). Accuracy of secondary structure and solvent accessibility predictions for a clostridial neurotoxin C-fragment. *Journal of protein chemistry*, 17(4), 311-318.
24. Rawlings, Neil D., Dominic P. Tolle, and Alan J. Barrett. "Evolutionary families of peptidase inhibitors." *Biochemical Journal* 378.3 (2004): 705-716.
25. Xu, R., & Xiao, Y. (2005). A common sequence-associated physicochemical feature for proteins of beta-trefoil family. *Computational biology and chemistry*, 29(1), 79-82.
26. Li, M., Huang, Y., Xu, R., & Xiao, Y. (2005). Nonlinear analysis of sequence symmetry of beta-trefoil family proteins. *Chaos, Solitons & Fractals*, 25(2), 491-497.
27. Huang, H., Qi, S. D., Qi, F., Wu, C. A., Yang, G. D., & Zheng, C. C. (2010). NtKTI1, a Kunitz trypsin inhibitor with antifungal activity from *Nicotiana tabacum*, plays an important role in tobacco's defense response. *FEBS journal*, 277(19), 4076-4088.